

Electronic Supplementary Information

Homogeneous synthesis of SiO₂@TiO₂ nanocomposites with controllable shell thickness and their enhanced photocatalytic activity

Yong Yu, Ming-Zhen Zhang, Jun Chen, and Yuan-Di Zhao*

*Britton Chance Center for Biomedical Photonics, Wuhan National Laboratory for Optoelectronics,
Department of Biomedical Engineering, Huazhong University of Science and Technology, Wuhan,
HuBei 430074, P. R. China.*

1. Experimental Section

1.1 Materials

The reagents used for the synthesis of SiO₂@TiO₂ were commercially available reagents. Tetrabutyl titanate, ethanol, acetic acid, sulfuric acid, tetraethyl orthosilicate, and Methyl Orange (MO) were purchased from Sigma-Aldrich. All the chemicals were used as received without further purification.

1.2 Characterization

The morphologies of all samples were observed by field-emission scanning electron microscope (SEM, JSM-6700F, JEOL, Japan). The structures of all samples were characterized with the aid of transmission electron microscope (TEM, Tecnai G20, JEOL, Japan). TEM EDX was used for the chemical analysis of samples. The composition of samples were measured by a powder X-ray diffractometer (XRD, D8 ADVANCE, Bruker, Germany) with Cu KR irradiation ($\lambda=0.15418$ nm).

1.3 Synthesis of SiO₂@TiO₂ composite

1.3.1 Synthesis of SiO₂

Monodispersed spherical SiO₂ nanoparticles were synthesized by the traditional Stöber method. Using a separatory funnel, 12 ml of ammonia was slowly fed into a reactor, in which a mixture of tetraethyl orthosilicate (10 ml) and ethanol (300 ml) had been loaded, followed by vigorous stirring for 24 h at room temperature. The precipitates were washed with ethanol, and then dried at 100 °C for 24 h.

1.3.2 Synthesis of SiO₂@TiO₂

The esterification of acetic acid with ethanol (molar ratio = 1:1) and hydrolysis of TiO₂ precursor was carried out in a round-bottom flask at 25 °C with SiO₂ (1 g), sulfuric acid (0.3 g), and tetrabutyl titanate (5 g) under moderate stirring after ultrasonic treatment. The collected precipitate

from reaction mixture after centrifugation was washed thoroughly with ethanol and dried at 110 °C overnight. The dried powder was put into Muffle furnace with crucible. After that, the temperature of Muffle furnace was increased from room temperature to planned temperature (*e.g.*, 500 °C) in air. When the calcination temperature reached planned temperature, Muffle furnace was kept at this temperature for 3 hours. Finally, sample was placed in vacuum oven for use after cooling.

1.4 Photocatalysis Measurement

MO solution (20 mg/L) was prepared in water, and 20 mL of the solution was transferred to quartz cuvettes. Control catalysts were placed in the cuvettes filled with MO solution. The quartz cuvettes were then exposed to UV light at room temperature. The decrease in absorbance of characteristic peaks of MO was measured after various reaction conditions using UV-vis absorbance spectroscopy. Absorbance measurements were recorded in the range of 200-800 nm, and the maximum absorption wavelength ($\lambda_{\max} = 462$ nm) for Methyl Orange was used for the calibration curves and further concentration measurements. The degradation efficiency catalyzed by SiO₂@TiO₂ was evaluated by the degradation ratio of MO which was calculated with the following formula: Decolorization = $[(C_0 - C)/C_0] \times 100$; where C and C_0 represent the time-dependent concentration and the initial concentration, respectively. In present study, all SiO₂@TiO₂ samples keep the constant weight and SiO₂ has various contents to explore the effect of SiO₂ loading on photoactivity.

$$\text{SiO}_2 \text{ loading (wt\%)} = \frac{\text{SiO}_2}{\text{SiO}_2 + \text{TiO}_2} \times 100\%$$

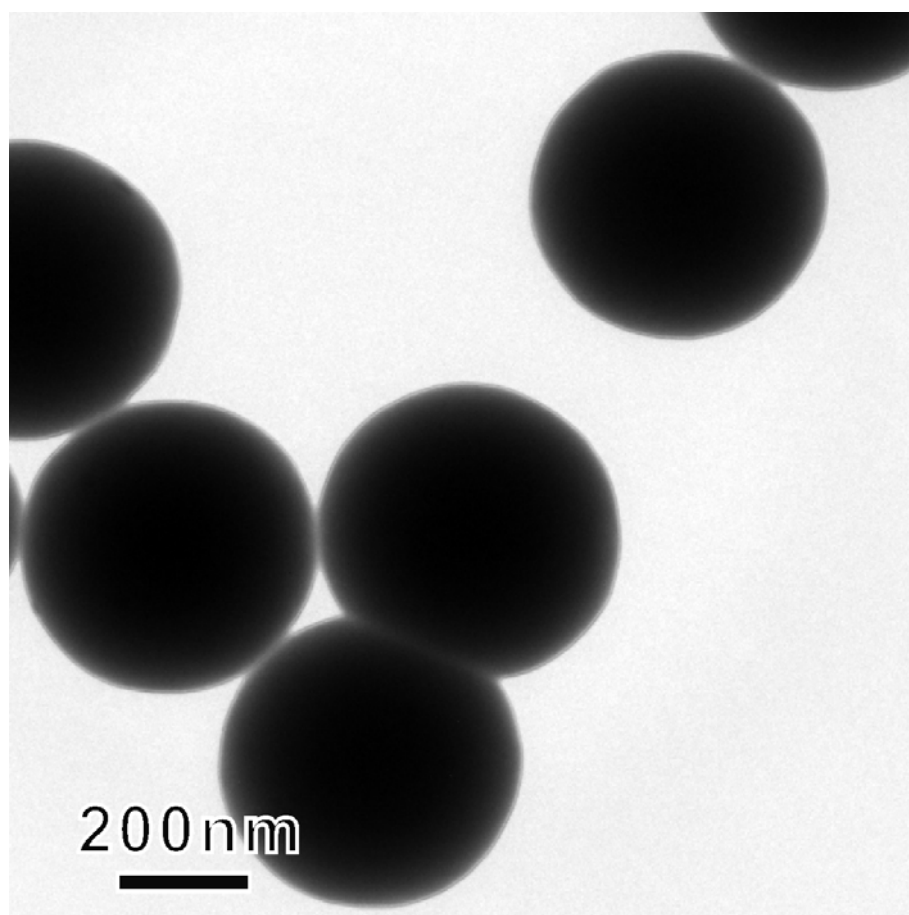


Figure S1. TEM image of SiO₂ NPs.

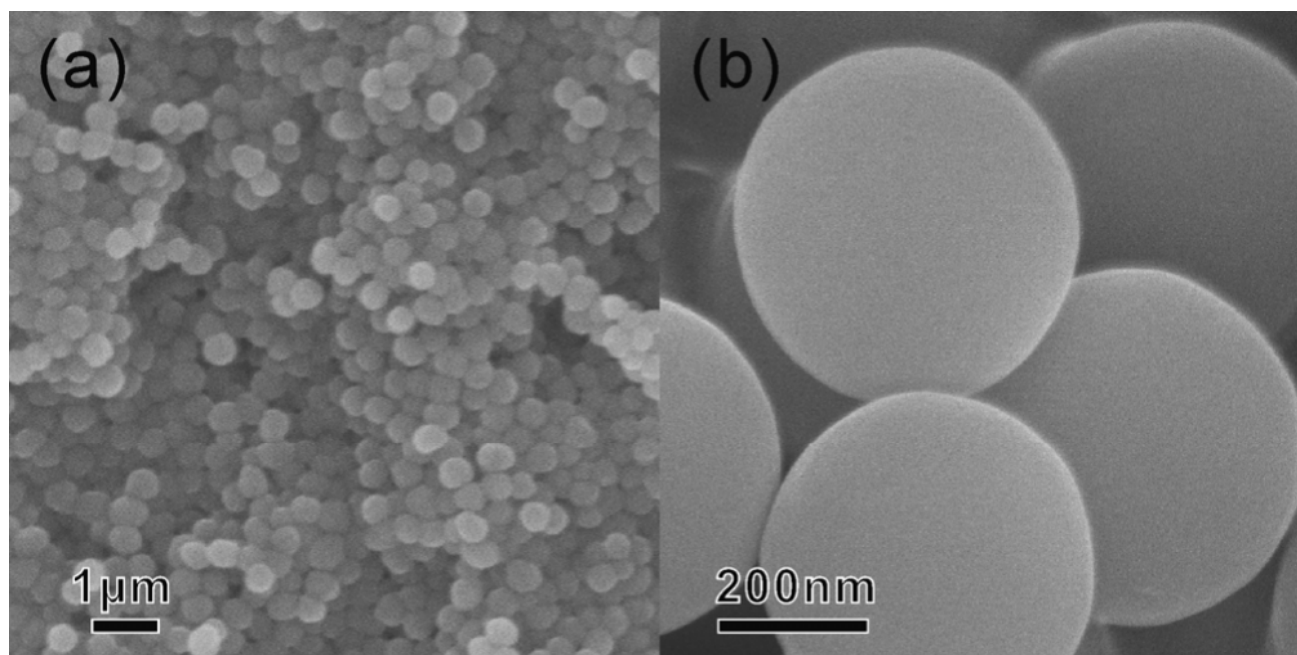


Figure S2. Low (a) and high (b) magnification SEM images of SiO₂ NPs.

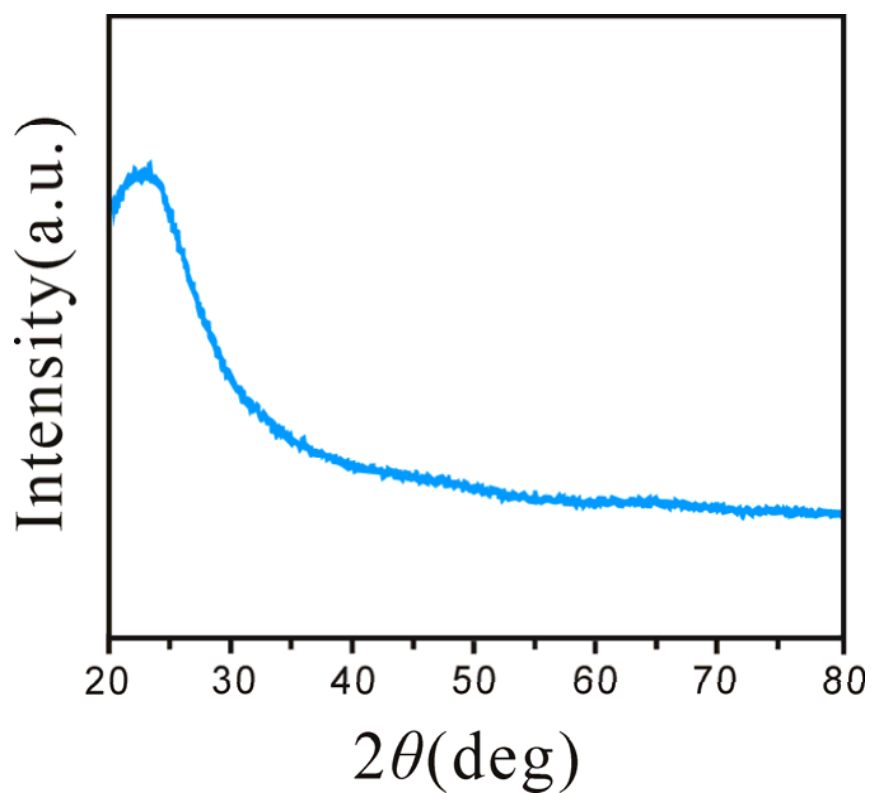


Figure S3. XRD pattern of SiO₂.

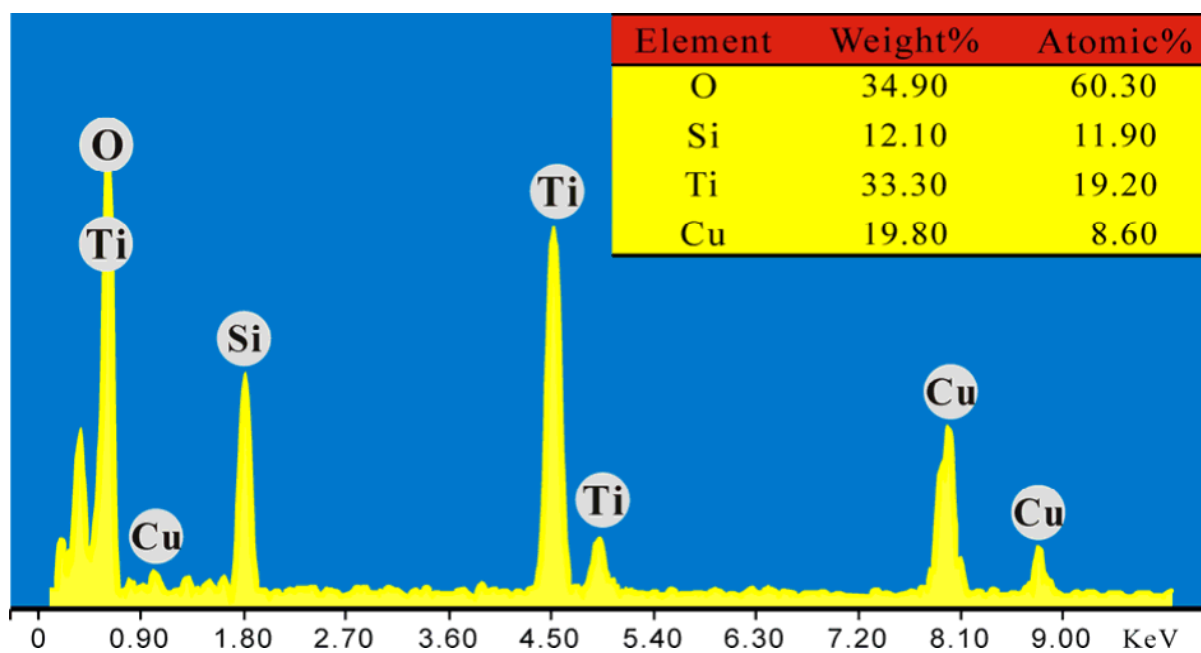


Figure S4. EDX spectrum of SiO₂@TiO₂.

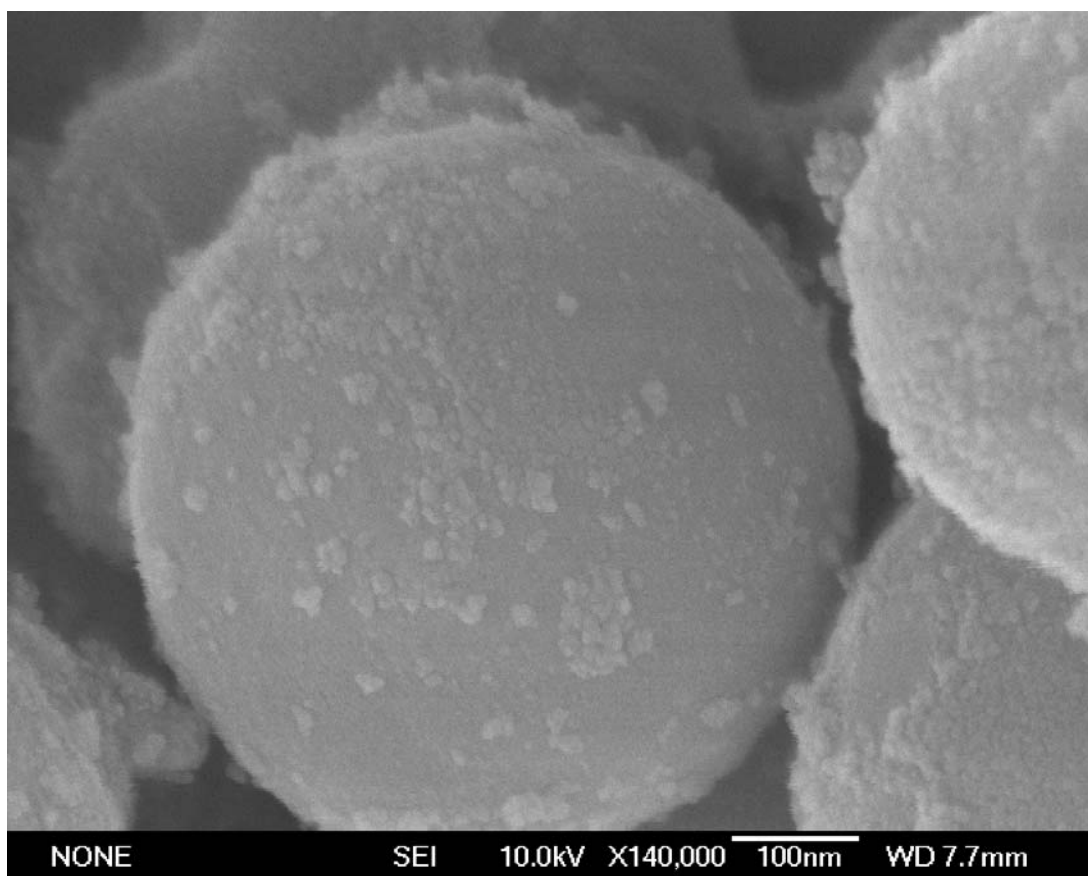


Figure S5. SEM images of $\text{SiO}_2@\text{TiO}_2$ after calcination.

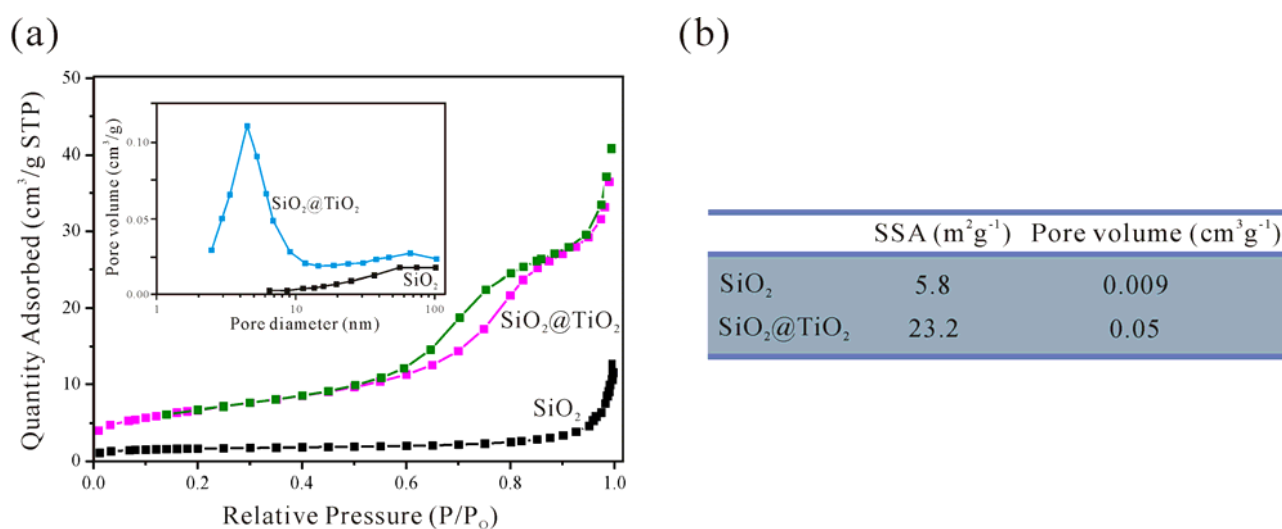


Figure S6. (a) N_2 adsorption and desorption isotherms of SiO_2 and $\text{SiO}_2@\text{TiO}_2$. Inset: Pore size distribution of SiO_2 and $\text{SiO}_2@\text{TiO}_2$. (b) Textural properties of SiO_2 and $\text{SiO}_2@\text{TiO}_2$.

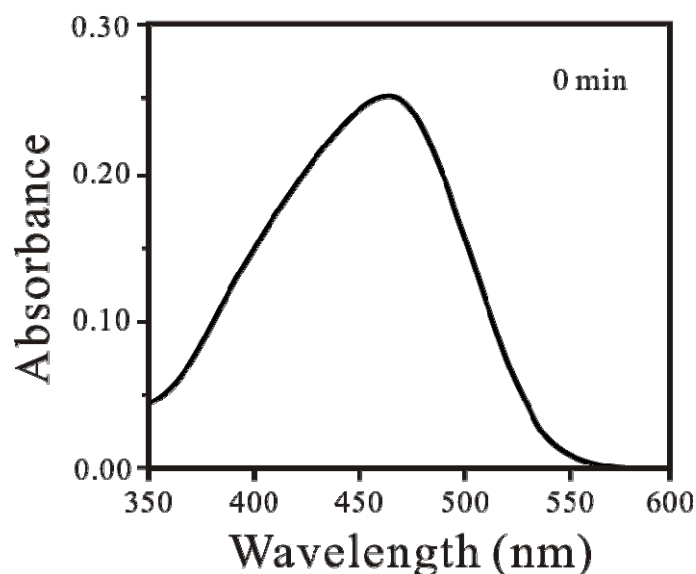


Figure S7. UV-vis absorption spectra of MO without catalyst at the beginning of experiment.

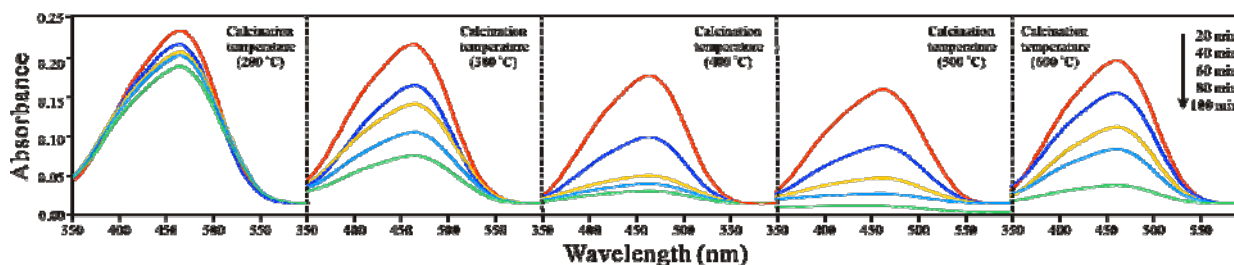


Figure S8. UV-vis absorption spectra of MO as a function of reaction time with various calcination temperatures of catalysts.

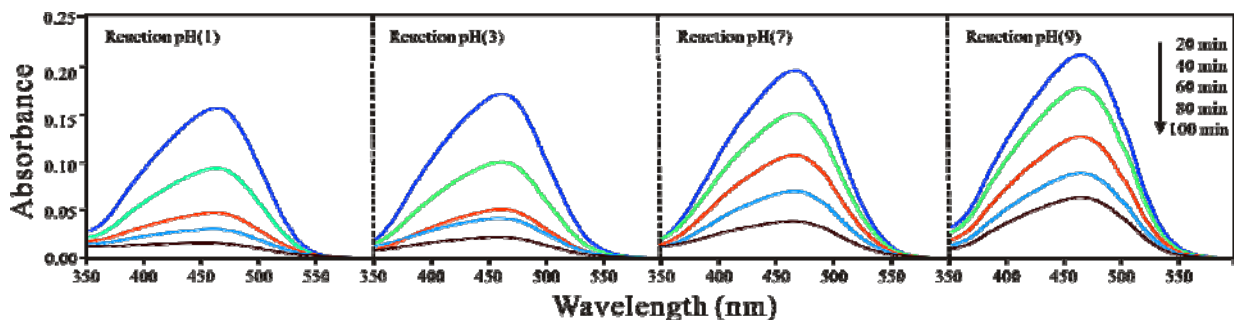


Figure S9. UV-vis absorption spectra of MO as a function of reaction time with various reaction pH.

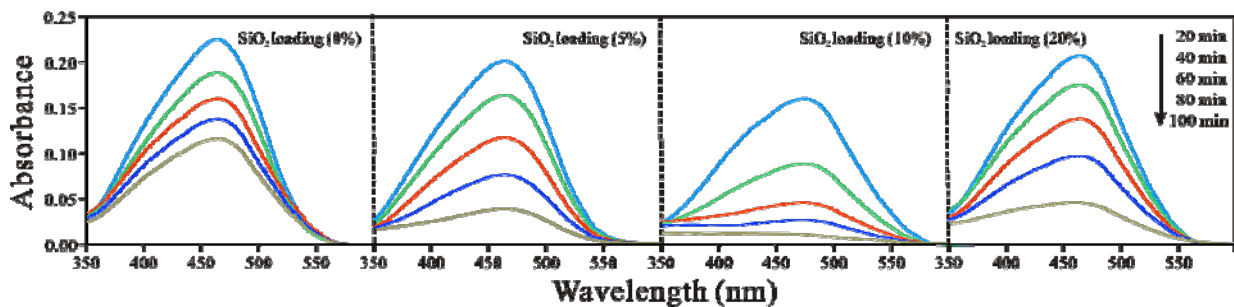


Figure S10. UV-vis absorption spectra of MO as a function of reaction time with various SiO₂ loading of catalysts.